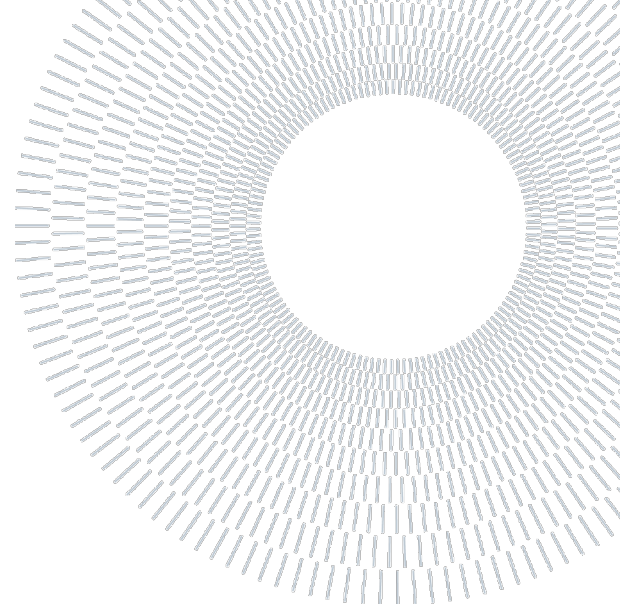




**POLITECNICO
MILANO 1863**

SCUOLA DI INGEGNERIA
CIVILE, AMBIENTALE
E TERRITORIALE



EXECUTIVE SUMMARY OF THE THESIS

Optimal sensor placement for structural health monitoring of communication towers

TESI MAGISTRALE IN Civile ENGINEERING – INGEGNERIA CIVILE PER LA RIDUZIONE DEL RISCHIO

Author: Arash Eisazadeh

Supervisor: Prof. Stefano Mariani

Co-supervisors: Prof. Alberto Corigliano and Ing. Elio Mariani

ACADEMIC YEAR: 2024-2025

Introduction

Structural Health Monitoring (SHM) has emerged as a critical approach to ensure the safety, serviceability, and sustainability of large-scale infrastructure. A fundamental component of SHM is Optimal Sensor Placement (OSP), which aims to minimize monitoring costs while maximizing the reliability and informativeness of collected data. Poor sensor placement can lead to incomplete or redundant information, significantly reducing the effectiveness of the monitoring system.

This thesis focuses on the application of SHM and OSP to communication towers, a class of tall, slender, and wind-sensitive structures of growing importance. The relevance of this work is underlined by the scale of the industry: Italy alone has more than 53,000 communication towers, while across Europe the number exceeds 500,000, and global market value is estimated at USD 80

billion by 2025, with annual growth above 10%. Companies such as INWIT are investing heavily in expanding tower networks, while operators already spend approximately 2–3% of annual revenues on inspections, maintenance, and upgrades.

Despite these investments, structural failures and downtime still pose significant safety and economic risks, particularly given the remote locations of many towers. Consequently, there is an urgent need for reliable, cost-efficient, and automated monitoring systems.

The primary objective of this thesis is twofold: first, to demonstrate the capability of SHM methods in detecting and localizing structural damage in communication towers. Second, to design and validate an optimized monitoring system based on a limited number of strategically placed sensors, ensuring accurate detection while minimizing costs. This dual focus reflects both the methodological contribution and the industrial significance of the research. The thesis is structured

to progressively develop the methodology, apply it to a real case study, and conclude with a validated optimal sensor layout.

Finite Element Modeling

The case study of this thesis is the EI Towers communication tower in Lissone (Italy), a self-supporting four-sided lattice tower with a total structural height of 76.24 m above base level. The finite element model was developed in SAP2000, with the tower discretized into 1144 joints and 2319 frame elements. with geometry, member properties, and loads defined in accordance with Eurocode provisions.

Tower geometry

Base dimension 7.0×7.0 m, tapering to 4.0×4.0 m at mid-height, 2.4×2.4 m in the upper-middle, and 1.4×1.4 m at the top. The tower consists of 1144 joints and 2319 frame elements, modeled with pinned connections and fixed-base supports. All members were modeled with beam/frame elements, pinned connections, and boundary fixity at the foundation. The segmentation of leg and bracing sections reflects the progressive reduction in stiffness with height, enabling efficient use of material while preserving stability. Figure 1 illustrates the actual tower at different elevations. Figure 2 shows the SAP2000 3D model [1], presenting the entire tower.

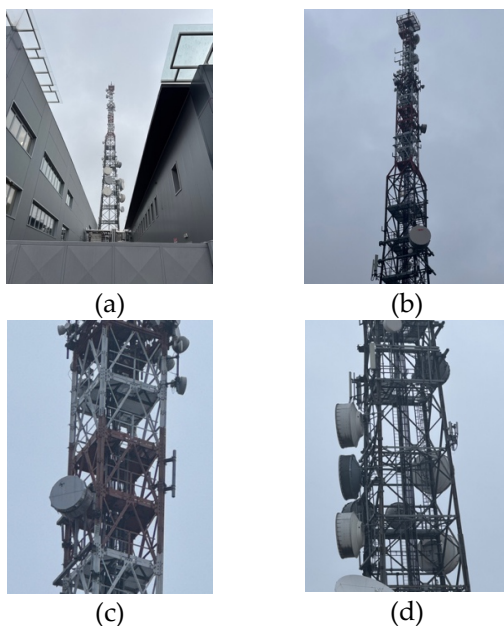


Figure 1. Views of the communication tower

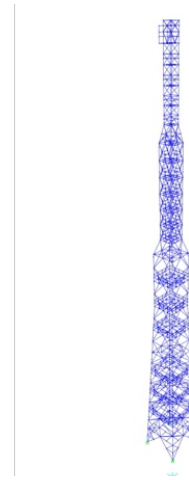


Figure 2. Overall view of the communication tower modeled in SAP2000.

Material properties and loading conditions

Material properties were assigned as S355 structural steel ($E = 2.1 \times 10^8$ kN/m², $\nu = 0.30$, $\sigma = 7850$ kg/m³, $F_y = 355$ MPa). Different profiles were used for legs, diagonals, and horizontals. Loads definition followed Eurocode EN 1991-1-4 [2]:

- Dead load: self-weight of the structure.
- Live load: 0.2 kN/m uniformly on antenna platforms and bracings.
- Wind load: modeled in three forms: equivalent static, response spectrum, and time-history (Eurocode-based turbulence)[2]:
 1. Static wind profile increases from 0.09 kN/m at the base to 0.45 kN/m at the top.
 2. Response spectrum defined according to Eurocode wind spectrum. presents the response spectrum function, where the horizontal axis represents the vibration period (s) and the vertical axis represents the spectral acceleration (m/s²).
 3. Time-history function generated from Eurocode spectrum and multiplied by the static distribution.

The mass source included full dead load plus $0.5 \times$ live load.

Modal and Dynamic analysis

Modal analysis extracted up to 200 modes, ensuring >90% cumulative mass participation in the two horizontal directions. The first frequency was $f \approx 0.88$ Hz (Figure 3), dominated by lateral bending, while the 200th mode reached a frequency of 30.03 Hz. The first seven modes captured ~85% of effective mass.

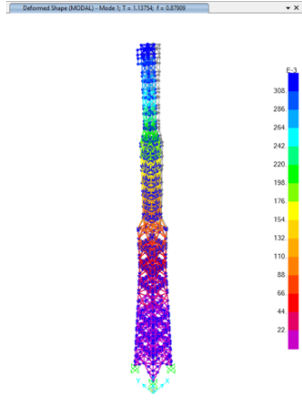


Figure 3. First eigenmode

Figure 4 shows deformed shape of the tower under wind response spectrum analysis. The contours show the maximum resultant displacement (in meters) obtained from the modal combination according to the response spectrum method. This represents the envelope of the structural response to turbulent wind loading. Time-history analysis captured transient displacement and acceleration series confirming that maximum displacements occur at the upper tower sections (Figure 4).

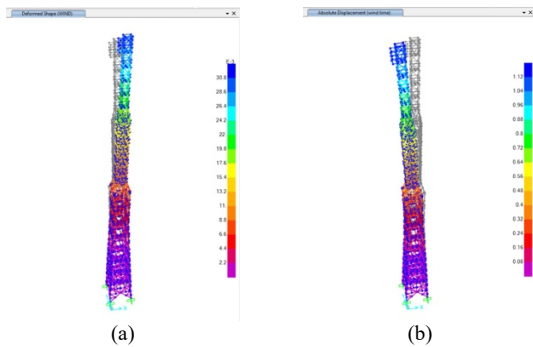


Figure 4. Maximum resultant displacement under dynamic wind load ((a) response spectrum, (b) Time-History)

Sensor Placement Methodologies

Three complementary methodologies for optimal sensor placement were adopted on the

communication tower: Effective Independence (EFI), Kinetic Energy (KE), and Proper Orthogonal Decomposition (POD). The objective was to identify the most informative degrees of freedom (DOFs) for installing sensors, ensuring that critical structural responses are captured with a limited number of devices.

Effective Independence (EFI)

EFI is a classical eigenmode-based method that maximizes the independence of modal information by optimizing the Fisher Information Matrix (FIM). Candidate DOFs are iteratively ranked, and those with minimal informational contribution are removed until the most informative set remains [3].

The formulation is based on the Fisher Information Matrix:

$$F = \phi^T M \phi \quad (1)$$

where ϕ is the modal matrix and M is the mass matrix.

The EFI index for the i^{th} DOF is:

$$EFI_i = \text{diag}(\phi(\phi^T M \phi)^{-1} \phi^T M) \quad (2)$$

In this study, the first seven mode shapes (from SAP2000 modal analysis) were used as input. The Top-100 DOFs were displayed on the tower model (Figure 6). EFI highlighted upper tower regions as dominant sensor candidates, providing a load-independent but modal-based perspective.

Kinetic Energy (KE)

The KE method prioritizes DOFs associated with the largest dynamic displacements and kinetic energy contributions. This increases resilience to sensor noise and emphasizes locations with stronger modal activity[4], [5].

The KE index is expressed as:

$$KE_i^{(n)} = \frac{1}{2} M_i (\phi_i^{(n)})^2 \omega_n^2 \quad (3)$$

Implementation used SAP2000 modal displacements and the mass matrix, processed in MATLAB. To obtain the total kinetic energy for

each DOF, the contributions across all seven modes were summed according to:

$$KE_i = \sum_{n=1}^7 KE_i^{(n)} \quad (4)$$

The top 100 DOFs were selected and visualized on the tower (Figure 6). Results confirmed that high-energy regions occur at mid-to-upper elevations.

Proper Orthogonal Decomposition (POD)

The POD is a response-based method that extracts dominant deformation patterns (POMs) from displacement time histories under wind loading. Given the snapshot matrix $X \in R^{m \times n}$ where each column is a displacement vector at time t_j , the decomposition is obtained via SVD[6]:

$$X = USV^T \quad (5)$$

The columns of U are the Proper Orthogonal Modes (POMs), and the eigenvalues of the covariance matrix.

$$C = \frac{1}{N} XX^T \quad (6)$$

determine the modal energy content. Wind time-history analysis generated displacement snapshots; POD via SVD showed that POM1 captured >99.9% of system energy. DOFs were ranked by their contribution to POM1, with the top 100 DOFs mapped to the tower (Figure 6). A comparison of POM1 vs. Eigen Mode 1 (Figure 5) revealed global bending similarities but also local differences at mid and top-sections, confirming POD sensitivity to load-dependent responses. This comparison is useful because it allows identifying structural areas that are more sensitive to actual wind excitation, thereby guiding more informed sensor placement and improving the effectiveness of monitoring strategies.

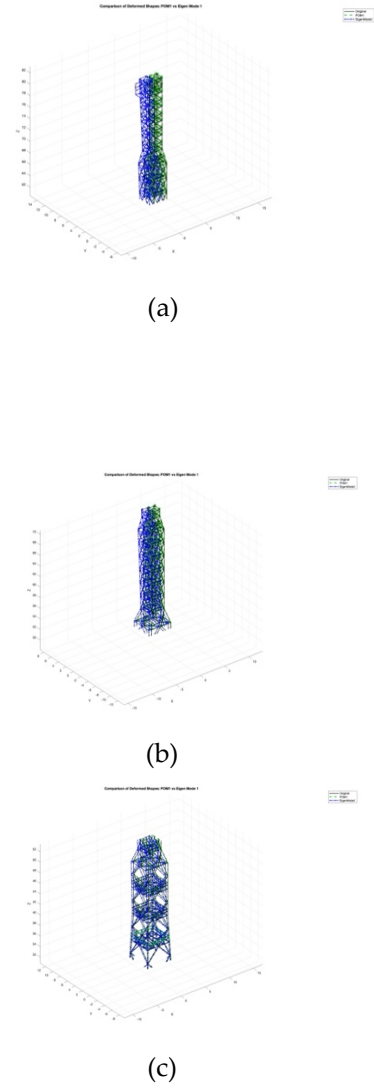


Figure 5. Comparison of POM1 vs. Eigen Mode 1 at different elevations

Superposition of Methods

To ensure robustness, EFI, KE, and POD results were superposed into a unified score:

$$S_i = \alpha \cdot EFI_i + \beta \cdot KE_i + \gamma \cdot POD_i \quad (7)$$

The top 100 DOFs with the highest cumulative scores were identified and displayed on the tower (Figure 6).

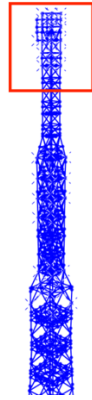


Figure 6. Top 100 DOFs ranked by KE method

The highlighted region corresponds to the upper part of the tower, where the most informative DOFs are consistently identified. The other methods (EFI, POD) also pointed to the same marked zone, confirming that this area is the most sensitive for sensor placement. This final distribution represents the most reliable set of candidate sensor locations, capturing both modal independence and load-specific response sensitivity. The results established a robust methodological framework for sensor placement. EFI provided load-independent modal coverage, KE emphasized high-response regions resilient to noise, and POD highlighted load-sensitive DOFs under wind excitation.

Damage Scenarios

The robustness of the proposed sensor placement strategies was evaluated under damaged configurations of the tower [7]. While before established candidate sensors in the healthy state, here the focus was on verifying whether these methods remain reliable when stiffness reductions are introduced. Sixteen scenarios were developed by removing selected bracing members across the tower height (upper, upper-middle, middle, lower-middle, and base). Braces were chosen due to their critical role in lateral stiffness and global stability. Damage was modeled symmetrically along the horizontal directions, aligned with wind load application. Figure 7 presents the four main damage zones along the tower.

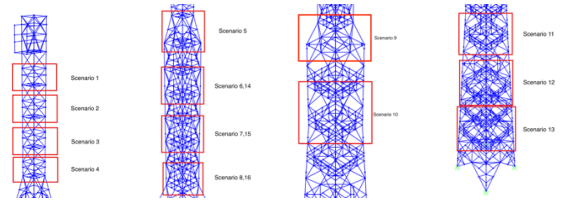


Figure 7. damage zones at different elevations

Each scenario includes: SAP2000 line information of removed members, pre-damage structural views (Figure 8) and eigenmode comparisons highlighting frequency/period shift. For example, in Scenario 10. The natural frequency changed from $f = 0.88$ Hz to $f = 0.74$ Hz.

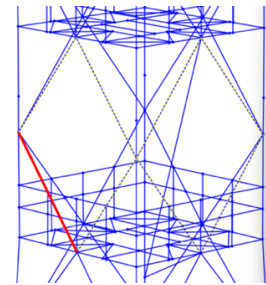


Figure 8. Pre damage with removed members highlighted – Scenario 10

Results showed that even localized removals produced measurable changes in the first eigenmode frequency and period, with severity strongly dependent on the location and number of removed members.

Application of Sensor Placement Methods

To assess sensitivity under damage, four methods were applied to each scenario:

MAC (Modal Assurance Criterion): quantified similarity between healthy and damaged eigenmodes. It is defined as [8] :

$$MAC_{i,j}(\Phi_i, \Phi_j) = \frac{|\Phi_i^T \Phi_j|}{(\Phi_i^T \Phi_i)(\Phi_j^T \Phi_j)} \quad (8)$$

where Φ_i and Φ_j are the mode shape vectors being compared. (e.g., Scenario 10 - Figure 9).

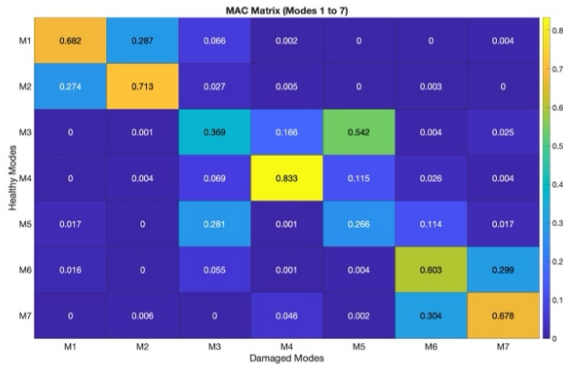


Figure 9. MAC for first seven mode (healthy Vs damaged) – Scenario 10

The results show that values close to 1 (yellow cells) indicate a strong similarity between the corresponding modes, while values near 0 (dark blue cells) reflect low correlation. Intermediate values (green-cyan) highlight partial similarity or mode mixing. As shown, most healthy–damaged pairs exhibit low MAC values, confirming that the structural damage caused significant changes in modal behavior. The diagonal dominance observed in some modes (e.g., Mode 4 with MAC = 0.833) suggests that while certain modes remain largely preserved, others are strongly affected or redistributed.

For each scenario, the following methods were applied, EFI ranked DOFs using modal observability, with results shown on the tower. POD extracted Proper Orthogonal Modes from displacement snapshots; POM1 consistently captured >99% of response energy, and comparisons with eigenmodes confirmed load-dependent deviations. Results were visualized on tower, KE ranked DOFs by modal kinetic energy contribution, with results presented on tower (Figure 10). A superposed index (E,q. 7) was then computed to consolidate rankings across methods, and also visualized on the tower (Figure 10). All these analyses were performed systematically for the healthy tower and for each of the 16 defined damage scenarios.

KL Divergence Analysis

In addition to EFI, KE, and POD, the Kullback–Leibler (KL) divergence method was implemented to quantify the statistical differences between the healthy and damaged structural responses. The KL divergence was then computed as [9]:

$$D_{KL} = (\mathbf{P} \parallel \mathbf{Q}) = \sum_i P(i) \log \frac{P(i)}{Q(i)} \quad (10)$$

where the summation index i runs over all Degrees of Freedom (DOFs) considered in the analysis, with $P(i)$ denoting the probability distribution of the response in the healthy state and $Q(i)$ the corresponding distribution in the damaged state. The KL divergence quantifies the dissimilarity between these two probability distributions: if the structure remains healthy, \mathbf{P} and \mathbf{Q} are nearly identical and the KL value is close to zero, while larger KL values indicate increasing deviations due to damage. To illustrate the procedure, one representative damage scenario was selected, and the results of all methods (EFI, KE, POD, Superposition, and KL divergence) were presented together (Table 1).

Table 1. KL-Divergences for each method in Scenario 10.

Method	EFI	POD	KE
KL Divergence	0.011252	1.46E-04	0.912866

KL divergence was computed across all methods to assess statistical differences between healthy and damaged responses. The KL divergence remains small across scenarios and methods this is expected given the very large number of DOFs and the near rigid-body-like behavior of the lower tower even with damage, displacements there change little. As a consequence, Methods are sensitive to the occurrence of damage (distribution shifts exist), but not strongly sensitive to its exact location unless the damage is sufficiently large to imprint a clear local signature.

Furthermore, for the same scenario, the 20 degrees of freedom that showed the largest differences between the healthy and damaged states for each method were highlighted and compared across all approaches, and their locations were displayed on the tower model, providing a clear example of how each technique identifies the most informative sensor positions (Figure 11).

Results and Discussion

The outcomes of all applied methodologies are consolidated and presented directly on the tower model, providing a spatial interpretation of structural sensitivity. The aim was to transition

from numerical indices (EFI, KE, POD and difference-based analysis) to visual mappings that highlight the most critical sensor locations. For each damage scenario (1–16) and each method (EFI, KE, POD, Superposition): Top 100 DOFs were shown in global views, illustrating the broader distribution of sensitivity across the tower height. Superposition of EFI, KE, and POD consolidated rankings into a combined index for robustness. (e.g. Scenario 10, Figure 10) Across most cases, the upper and upper-middle regions concentrated the highest EFI and POD ranked DOFs, consistent with wind-induced deformation patterns. Top KE values extend more widely along the height of the tower. In addition to the sensitivity rankings, the 20 DOFs with the largest differences between healthy and damaged states were also mapped on the tower for each method and scenario. This highlights the locations where the damage produced the most pronounced effect in terms of variation in the sensitivity indices. By combining the top 100, and top 20 difference based DOFs, a comprehensive picture of structural sensitivity is obtained for each damage case. These visualizations not only confirm the results of the numerical analyses but also provide a clearer spatial understanding of how damage influences different regions of the tower.

Finally, these results form the foundation for determining the optimum number and placement of sensors. The sensor layout will be designed to maximize the capture of structural responses in the most critical regions. Furthermore, the type of sensors and their required sensitivity will be defined based on the local displacement amplitude at the selected installation points, ensuring that the chosen configuration is both technically effective and practically feasible. In addition, the sensor design should also be evaluated in terms of the value of information (VoI). This concept reflects how much each additional sensor contributes to reducing uncertainty and improving damage detectability. From this perspective, the comparison of different methods is particularly meaningful, as it allows the identification of non-redundant yet informative regions across the tower—areas that provide unique contributions to increasing the overall value of information of the monitoring system. If too many sensors are concentrated in the same region, they tend to provide redundant data without adding

significant new knowledge. As observed in stochastic OSP formulations, VoI increases with the number and quality of sensors, but at a decreasing rate: once a sufficient number of sensors has been deployed, adding further sensors yields only marginal improvements [10].

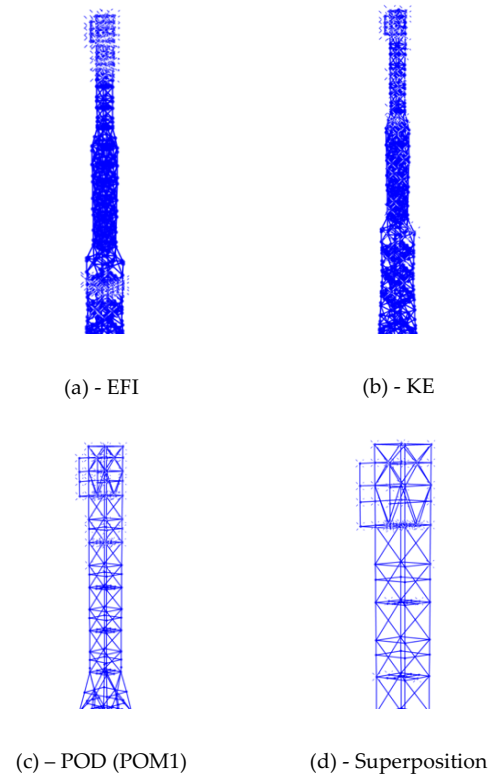
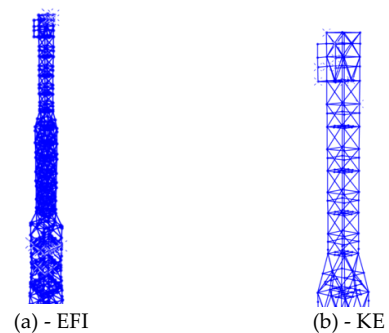


Figure 10. Top 100 DOFs for each method on tower – Scenario 10



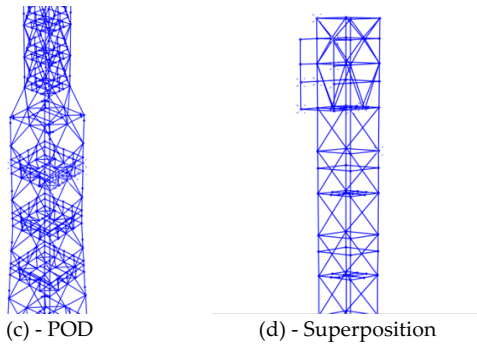


Figure 11. Top 20 largest difference in value of each method (healthy Vs damaged) – Scenario 10

Conclusions

This thesis investigated the objective of optimal sensor placement and damage localization on a communication tower under wind loading. To address this objective, three methods were applied: EFI, KE, and POD (with a superposed index). In practice, many industrial approaches rely on placing a single accelerometer at the top of the tower, since that is where maximum displacement occurs. While this configuration captures global vibration trends, it cannot reliably detect all damage scenarios. On the other hand, installing sensors along the entire tower height would in principle allow detection of any damage location, but this solution is prohibitively expensive in terms of both sensor hardware and data analytics. The strategies applied in this thesis—EFI, KE, and POD, along with their combinations—represent well-established approaches for sensor placement and damage detection. EFI is an eigenvalue-based method that ranks DOFs by their independence in capturing mode shapes. KE highlights DOFs with the highest modal energy contribution. POD is a data-driven technique that extracts dominant patterns from structural responses under wind loading. EFI and KE provide mode-shape-based insights, which are independent of the applied loading, while POD incorporates response data, and their combination offers a balanced and practical compromise. With a limited number of sensors placed in optimal locations, it is possible to achieve high sensitivity to damage while minimizing system complexity and cost.

Key findings

The results of the different methods provide several important insights into the effectiveness of

sensor placement strategies for damage detection and localization on the tower. All methods were able to reliably indicate the occurrence of damage by highlighting differences between the healthy and damaged states. However, their ability to precisely localize the damage strongly depended on the severity and the location of the damage. In the severe damage scenarios (Scenarios 6–8), all methods showed clear peaks at the damaged region, directly capturing the affected zone. For other scenarios, the difference-based POD analysis demonstrated superior localization capability, as the most affected DOFs consistently clustered at the actual damage floor or within one story above or below it. In contrast, EFI provided a coarser localization, while KE exhibited a broader but complementary distribution of informative DOFs. Under typical wind responses, EFI and POD rankings were dominated by upper and upper-middle DOFs, whereas KE tended to distribute informative points more widely along the tower height.

The relatively small KL divergence values do not indicate a lack of sensitivity but rather reflect the combined effect of the large number of DOFs and the near-rigid behavior of the lower part of the tower, where even substantial damage produces only minor relative variations. Accelerometer responses further confirmed the occurrence of damage, but the ability to identify its exact location varied depending on the severity and position of the scenario: strong or well-positioned damage could be detected with high accuracy, while smaller or lower-level damages were harder to pinpoint. Among the methods studied, the difference-based POD analysis consistently achieved the best localization accuracy, confining the damaged region within approximately one story of the actual member. Difference-based EFI and KE localized the damage with a broader range, typically 40–50 m, yet even this resolution represents a substantial improvement compared to the need for inspecting the full tower height.

Recommended sensor layout

In the proposed monitoring strategy, POD was applied to accelerometer data as the core analytical engine. A baseline representation was first established under healthy conditions, which then served as the reference for detecting damage. Deviations were identified through changes in the

spectral content and in the distribution of modal contributions, while localization was achieved by examining the top 20 DOFs that exhibited the largest differences in POM1 values. To translate these findings into a practical sensor placement scheme, sensors were positioned every other floor and mirrored on opposite faces of the tower to account for structural symmetry (Figure 12). This workflow reduces inspection from the entire 70 m height to a narrow floor band (± 1 floor), improving efficiency and cutting costs, while ensuring that critical damage is not missed. Even though the methodology does not always identify the exact member where the damage occurred the approach effectively narrows the inspection scope:

- EFI and KE reduce the search area to 40–50 m of tower height.
- Difference based-POD analysis further improves this, limiting the damage zone to just one floor above or below the actual damaged member (e.g., from the entire tower height down to a few floors).

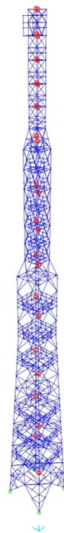


Figure 12. Final Proposed Sensor Placement

This represents a significant practical advantage for maintenance activities, enabling targeted inspections rather than full-scale climbing and checking of all members. This allows engineers to focus their inspections more efficiently, saving both time and cost. Despite these advantages, some limitations remain. For instance, localization accuracy decreases under very light damage,

measurement noise and environmental variability were not explicitly modeled, and the iFEM method could not be directly implemented since SAP2000 does not provide stiffness matrix.

Future work

Building on the findings of this study, several directions for future research can be outlined. A natural extension would be to consider multi-directional wind loading cases together with varied turbulence realizations, in order to more realistically capture the environmental conditions acting on the tower. Experimental validation on a real structure is also essential, as it would allow the robustness of the proposed strategies to be tested against measurement noise and operational variability.

Another promising direction is the integration of artificial intelligence for sensor placement refinement. AI-based optimization could help identify sensor layouts that further balance accuracy and efficiency. Similarly, the application of the Inverse Finite Element Method (iFEM) represents a valuable opportunity, the informative points identified by EFI, KE, and POD could serve as virtual measurement inputs for iFEM, enabling the reconstruction of the full displacement field of the tower. By comparing reconstructed responses with the original finite element model, the informativeness of each candidate sensor set could be quantified, ultimately leading to a more optimal and reliable sensor configuration. Finally, vision-based monitoring systems could be explored as a complementary approach. Installing a camera at a fixed external location with a complete view of the tower would enable continuous, non-contact tracking of global displacements through image or video processing. Such a system could enhance redundancy, extend monitoring capabilities to degrees of freedom that are difficult to instrument with accelerometers, and further strengthen the overall reliability of the monitoring framework.

Finally, a promising avenue would be the practical deployment of a wireless sensor network. A possible configuration would include two slave nodes mounted on opposite faces of the tower, each equipped with three tri-axial accelerometers (aligned with the global X, Y, and Z directions), an Arduino board for sampling and preprocessing, and a ZigBee transceiver for wireless data

transmission. Implementing and testing such a system on a real tower would provide valuable insights into the practical feasibility and long-term performance of the proposed strategies.

Broader Implications

This research challenges the industry practice of monitoring only the tower top and demonstrates the benefits of optimized distributed monitoring. By reducing the required number of sensors while improving localization accuracy, the approach offers a low-cost and efficient SHM strategy. Furthermore, the methodology can be extended beyond communication towers, with strong potential applications in other infrastructures such as bridges, where reliable SHM remains a pressing need.

Acknowledgements

I would like to express my sincere gratitude to my supervisor, Prof. Stefano Mariani, for his invaluable guidance and continuous support throughout this thesis. I am also grateful to my co-supervisors, Prof. Alberto Corigliano for his constructive feedback and kind assistance, which greatly enriched the quality of this work. Finally, my special thanks go to Ing. Elio Mariani and EI Towers for providing the tower design and essential support that made this study possible.

References

- [1] "Home - SAP2000 - CSI Knowledge Base." Accessed: Sep. 02, 2025. [Online]. Available: https://web.wiki.csiamerica.com/wiki/spaces/sap2000/overview?homepageId=1802245&utm_source=
- [2] "EN 1995-1-1: Eurocode 5: Design of timber structures - Part 1-1: General - Common rules and rules for buildings," 2004.
- [3] D. C. Kammer, "Sensor placement for on-orbit modal identification and correlation of large space structures," *Journal of Guidance, Control, and Dynamics*, vol. 14, no. 2, pp. 251–259, May 1991, doi: 10.2514/3.20635;PAGE:STRING:ARTICLE/CHAPTER.
- [4] Z. Su, L. Ye, and Y. Lu, "Guided Lamb waves for identification of damage in composite structures: A review," *J Sound Vib*, vol. 295, no. 3–5, pp. 753–780, Aug. 2006, doi: 10.1016/J.JSV.2006.01.020.
- [5] M. Meo and G. Zumpano, "On the optimal sensor placement techniques for a bridge structure," *Eng Struct*, vol. 27, no. 10, pp. 1488–1497, Aug. 2005, doi: 10.1016/J.ENGSTRUCT.2005.03.015.
- [6] S. Eftekhar Azam, "Online Damage Detection in Structural Systems," *SpringerBriefs in Applied Sciences and Technology*, no. 9783319025582, p. 135, 2014, doi: 10.1007/978-3-319-02559-9.
- [7] S. Hassani and U. Dackermann, "A Systematic Review of Advanced Sensor Technologies for Non-Destructive Testing and Structural Health Monitoring," *Sensors 2023, Vol. 23, Page 2204*, vol. 23, no. 4, p. 2204, Feb. 2023, doi: 10.3390/S23042204.
- [8] "The modal assurance criterion - Twenty years of use and abuse | Request PDF." Accessed: Sep. 04, 2025. [Online]. Available: https://www.researchgate.net/publication/296949512_The_modal_assurance_criterion_-_Twenty_years_of_use_and_abuse
- [9] S. Kullback and R. A. Leibler, "On Information and Sufficiency," *The Annals of Mathematical Statistics*, vol. 22, no. 1, pp. 79–86, Mar. 1951, doi: 10.1214/AOMS/1177729694.
- [10] G. Capellari, E. Chatzi, and S. Mariani, "Structural Health Monitoring Sensor Network Optimization through Bayesian Experimental Design," *ASCE ASME J Risk Uncertain Eng Syst A Civ Eng*, vol. 4, no. 2, p. 04018016, Mar. 2018, doi: 10.1061/AJRUA6.0000966.